New Approach for Making Standard the Development of Biosensing Devices by a Modular Multi-Purpose Design

New Approach for Making Standard the Development of Biosensing Devices by a Modular Multi-purpose Design

Abuduwaili Tuoheti, Simone Aiassa, *Student Member, IEEE,* Francesca Criscuolo, *Student Member, IEEE,* Francesca Stradolini, Ioulia Tzouvadaki, Sandro Carrara, *Fellow, IEEE,* and Danilo Demarchi, *Senior Member, IEEE*

***Abstract*—The fast widening of biosensing applications, such as healthcare, drug delivery, food, and military industries, is increasing the need for generality and compatibility among different sensors. To address this challenge, we present here an innovative approach for the fast development of new electronic biosensing systems, linking a custom-designed front-end with a multi-purpose system. We envision an open tool to help designers to focus on the target molecule and related detection method instead of designing each time a dedicated electronic device. The architecture of the proposed system is based on a modular approach, where only the front-end and the software need to be custom re-designed according to the application. Considering current research and applying a rigorous definition of the technical requirements, the core of the system is designed to fit the highest number of biosensing methods. The flexibility of this approach is successfully demonstrated with three different types of biosensors, i.e., amperometric, ion-sensitive, and memristive.**

***Index Terms*—Biosensor, Electrochemical sensing, General-purpose, Ion-sensor, Memristive, Open-source.**

I. Introduction

BIOSENSORS are being widely adopted in biomedical diagnosis, point-of-care systems, food industry, environmental monitoring, water quality measurements, prosthetic devices, and drug discoveries [1]. The term biosensor defines a device which combines a biological component with a physicochemical system for the detection of a chemical substance [2]. Namely, the biosensor outputs the presence and the quantity of the target molecule. According to the definition, the world of biosensors is an extensive collection of systems and devices, which exploit different working principles depending on the different target molecules [3], [4]. Just to list some examples, biosensors could leverage on electrochemistry [5], acoustic techniques [6], surface plasmon resonance [7], or luminescent principles [8]. Due to the large variety of biosensing techniques, it is not possible to develop a system capable of interfacing with all types of biological detector. Regardless, standardization is crucial to help the growth and spread of the technology [9], being the compatibility the main driver to the envisioned era of Internet of Things (IoT) sensor networks [10]. In this context, there is an increasing interest in the design of more generalized biosensing platforms [11] or multi-purpose sensing devices [12]. The development of a low-cost general application potentiostat is a critical challenge [13] and the research is pushing towards the development of open source systems, like open-source potentiostats [14], [15], [16] in the effort of giving to the scientific community flexible instruments to develop new sensing platforms with reduced deployment cost and time. Open-source hardware would contribute to foster the growth of the IoT sensors, reducing present barriers and advancing in technologies [17], especially if suitable for diversified biosensing devices. Nevertheless, to the best of our knowledge, up to now published open architectures only implement potentiostats without considering the processing of the information [13], [14], [15], [16]. Consequently, the output is the electrochemical signal, not the actual analyte concentration. For this reason, there is the subsequent need to process offline the data after the acquisition of the measurements.

On the other hand, the majority of the biosensing circuits presented in literature still target a specific application. For example, in drug delivery applications, biosensing platforms are used as low-cost, low-power, and reliable devices to measure the concentration of molecules delivered to patients or to provide continuous monitoring of the health status [18]. For those applications, amperometric sensors are widely adopted since they offer a fast and reliable procedure for detecting the target molecule [19], [20], [21]. In health-monitoring, biosensors have been used in sports practices as there is the need to evaluate and monitor biological parameters of the athlete, estimating fatigue and health status [22], [23]. Those measurements are carried out through potentiometric sensing [24]. Aptamer-based memristive biosensors are employed in early-stage cancer diagnostics to provide ultra-sensitive detection for cancer markers [25].

Since all the literature examples mentioned above are custom-developed, each device needs dedicated hardware to drive the sensor and read the measurements. In those examples, the requirements of portability, low-cost or low-power demand custom electronics and dedicated software, which limit the

Manuscript received Jan 27, 2020; accepted May 13, 2020. Date of publication –; date of current version May 14, 2020. The associate editor coordinating the review of this paper and approving it for publication was Dr. Dan Nicolau. *(Abuduwaili Tuoheti and Simone Aiassa contributed equally to this work) (Corresponding author: Simone Aiassa).*

A. Tuoheti, S. Aiassa, and D. Demarchi are with Department of Electronics and Telecommunications, Politecnico di Torino, Turin 10129, Italy, and also with Integrated Systems Laboratory, École Polytechnique Fédérale de Lausanne, Lausanne 1015, Switzerland (email: simone.aiassa@polito.it).

F. Criscuolo, F. Stradolini, I. Tzouvadaki, and S. Carrara are with Integrated Systems Laboratory, École Polytechnique Fédérale de Lausanne, Lausanne 1015, Switzerland.

usage of commercially available systems. Many biosensors in literature have in common the need to correctly apply and read a voltage or a current signal. Moreover, all these electronic biosensor devices need to integrate a human interface to configure and control the system efficiently and to display in comprehensive and readable way the results, meanwhile everything has to be integrated into a single object. In this work, we take advantage of these similarities to demonstrate a generalized electronic system that can be easily extended to a considerable number of applications. A new multi-purpose system is proposed in the effort of giving the scientific community an open tool for new devices without focusing on the complete design path. In particular, this work proposes a modular system that provides the possibility of creating a brand-new entire biosensor electronic device by merely adding a custom front-end module to a general-purpose system, and writing a firmware/software. This simplification may help the designers to focus only on the specific target molecule design peculiarities for the sensing platform. In our approach, the designers have still to develop one of the most challenging part, i.e. the transducer and the signal conditioning. However, when they overcome this barrier, our system may provide them with a way to quickly exit the lab environment and to enter in the field with a complete and integrated biosensor electronic device, without commercial systems.

In order to demonstrate the capability of our approach, the presented system is tested with three example applications, exploiting different detection methods. The first example is based on an amperometric method for drug detection, the other one leverage on a potentiometric technique for ion sensing, and the last example employs a memristive sensor for cancer markers detection. All devices are developed upon the common general-purpose platform defined in this work, and they share with each other most of the system.

The paper is organized as follows: In Section II, we present the approach. A detailed description of our architecture and its hardware implementation is exposed in Section III. Section IV shows three examples of complete biosensing devices to demonstrate the capability of our approach. Section V describes the materials and methodology used for the validation of the system. The experimental results and discussion are presented in Section VI. Finally, Section VII reports the conclusions.

II. The Approach

The biosensor is a device detecting analytes in biomedical/biochemical applications, measuring their concentration and/or recognizing their structure, compositions and functions. Typically, a biosensing device consists primarily of a transducer where the bio-chemical information is converted into an electrical signal. In some cases, the biosensor needs a stimulus to enhance or activate a chemical process. In order to read the signal produced by the transducer, a front-end circuit must be provided. This module is responsible for signal conditioning, amplification, conversion, range matching, and filtering [1], [26]. The back-end controls the sampling of the electrical signal with analog to digital conversion, usually, adding digital filters. The back-end is also driving the sensor front-end with excitation or stimuli. The samples acquired by the back-end are generally processed by a core, able to convert the rough sampled information into a result, which is the final measure of the target molecule.

To implement of our general-purpose system, many examples in literature [19], [20], [21], [22], [25], and many review-papers [3], [18], [4], [6], [7], [8], [24], [25], have been methodically analyzed to define the technical requirements for fitting to the highest possible number of applications. The device is divided into its three parts (front-end, back-end, and core) and the parts requiring to be application-specific customized are carefully separated from the rest of the system. Fig. 1 shows the approach, depicting a possible stacked implementation. While the top module, i.e. the front-end, must be designed each time according to the target biological compound, the middle module and the bottom module (back-end and core) need only to customize the firmware and the software, respectively.

The connection between front-end and back-end is the novelty of the proposed system because we recognize in this point, the boundaries between custom and general. Hereof, after defining the technical requirements and specification derived from literature, a general-purpose port is designed to enable the implementation of the proposed system in multiple and not-limited numbers of biosensing device, giving great flexibility to the final user.

III. The System

We aim to design a flexible, modular, and easy-to-use general system to help fast development of biosensing devices. As a result, the actual design of the platform is based on an embedded system. Fig. 2 shows the architecture of our system, which contains three modules, the front-end the back-end and the core specified in our approach. The back-end module measures the incoming electrical signal from the electronic biosensor in the front-end; it converts the signal to digital data through the sampling and stimuli block. Besides, it provides the data via a Micro Controller Unit (MCU) to the core for

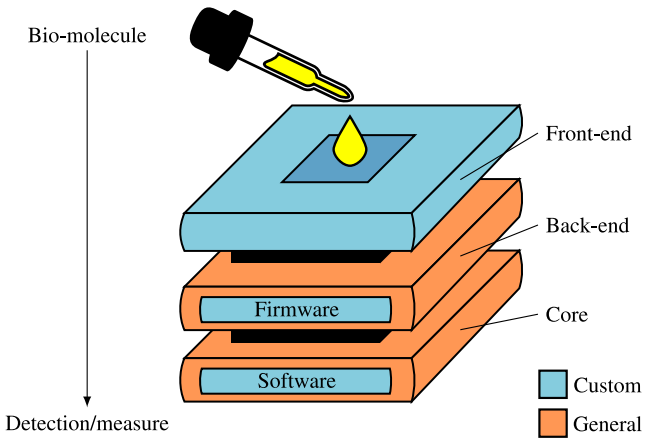

Fig. 1. Stucture of a biosensing device according the proposed approach. The custom front-end is the bio-interface (top), the general back-end (middle) and core (bottom) manages with custom firmware and software the sampling and the processing.

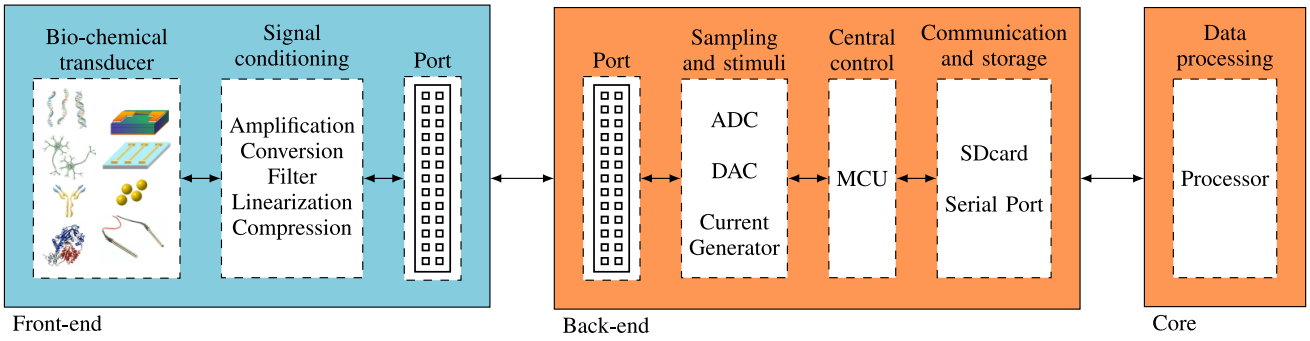

Fig. 2. Overall architecture of the embedded system according to our approach. The custom front-end (left) interfaces through a general back-end (centre) and a processing core (right).

processing and cloud connection. The port connects the front-end to the back-end, it powers up the electronic biosensor, it acquires the desired measured signal through its address lines, and it provides the clock signal if needed on the front-end side. The core block controls the interfacing with the cloud server, and it is responsible for data analysis. As per its structure and features, our developed system is application-flexible as it is intended to support an extensive number of sensing techniques targeting a wide range of biological compounds. Furthermore, the system is implemented to be portable, easy to use, and programmable. To address some of the major challenges in biosensors, such as varying sensitivity levels based on ambient conditions (like humidity and temperature), we added temperature and humidity sensor directly on the back-end.

A. Front-end

To enlarge system applicability to various types of biosensing techniques, we need here to define and specify the technical requirements for the front-end. This module needs to be connected, on one side, with the biological sample where the target molecule is measured and on the other side with the back-end. Therefore, it needs on-board all the electronic functions for this aim. The front-end has to satisfy the following requirements:

1) It is based on particular biological material or organic membrane selective and specific for the sensing.
2) It contains at least one transducer that translates the target biochemical information into an electrical signal.
3) It conditions the electrical signal to be compatible with the back-end.
4) If required, it includes all the component to stimulate or excite the desired chemical reaction.
5) It interfaces to the back-end according to the port defined in this work.

B. Back-end

The back-end is the first module provided to the final user not requiring to be customized apart from the firmware. The module contains the port to be interfaced to the front-end, a sampling and actuation block, a central control block and a storage and communication block.

1) Sampling and stimuli: The sampling and stimuli block consists of an Analog to Digital Converter (ADC), four Digital to Analog Converters (DAC) and a current generator block. All components for sampling and stimuli communicate through a Serial Peripheral Interface (SPI) standard protocol. The $24\,\mathrm{bit}$ Analog Devices LTC2380-24 ADC measures the input signals featuring an high accuracy and single input channel with $1.5\,\mathrm{Mbps}$ of sampling frequency, $28\,\mathrm{mW}$ of power consumption, Integral Non-Linearity (INL) of $\pm 3.5\,\mathrm{ppm}$, and no missing codes at $24\,\mathrm{bit}$. The DAC is a $16\,\mathrm{bit}$ 4 channel Analog Devices AD5686R with high relative accuracy ($\pm 2\,\mathrm{LSB}$, Least Significant Bit) maximum at $16\,\mathrm{bit}$ and a $2.5\,\mathrm{V}$, $2\,\mathrm{ppm/°C}$ reference. The on-board microcontroller features an internal $12\,\mathrm{bit}$ ADC and a $12\,\mathrm{bit}$ DAC. The current generator block is designed to generate currents at 4 different ranges, i.e., $0\,\mathrm{nA}$ to $1\,\mathrm{nA}$, $0\,\mathrm{nA}$ to $100\,\mathrm{nA}$, $0\,\mu\mathrm{A}$ to $100\,\mu\mathrm{A}$ and $0\,\mathrm{mA}$ to $25\,\mathrm{mA}$. It is composed of a DAC and a voltage to current conversion circuit, with the 4 current ranges mentioned above.

2) Central control: In our implementation, the control block in the back-end is based on an STMicroelectronics STM32F769BGT6 Micro-Controller Unit (MCU). The MCU is selected because of its internal hardware resources, high performance with $216\,\mathrm{MHz}$ clock frequency and power management modes for low power applications. The MCU is responsible for processing commands and data with other peripherals. The system includes the possibility of measuring humidity and temperature of the surrounding environment from an Adafruit Sensirion SHT31-D temperature and humidity sensor module, which provides a $\pm 2\,\%$ relative humidity accuracy and $\pm 0.3\,°\mathrm{C}$ temperature accuracy.

3) Communication and storage: During the measurement, the acquired data are transferred to the core module through a standard serial UART port. The serial port communicates up to a baud rate of $460.800\,\mathrm{bit}$ per second to support measurements with strict timing constraints. The measurement data can also be stored directly into a micro SD card that can be inserted in its slot on the back-end.

C. Port

The general-purpose port acts as a bridge in interconnecting the front-end and the back-end. The port is composed of $26\,\mathrm{pin}$ to give high flexibility, and it also provides the power supply and the control signals to the front-end. In the port,

four voltage supply lines, namely, $\pm 3.3\,\mathrm{V}$ and $\pm 5\,\mathrm{V}$, with a ground line, are included, as these voltage levels are most common in biosensing applications. The Voltage Input (VI) pin is connected to the ADC present on the back-end module. Four Current Input pins (IOA, IOB, IOC, and IOD) and four Voltage Output pins (VOA, VOB, VOC, and VOD) connect the four current ranges coming from the current generator and the four DAC voltage outputs in the back-end module. Four selection pins (SEL1, SEL2, SEL3, and SEL4) provide the capability of adding a sixteen to one analog multiplexer on the front-end to the benefit of a multiplexed array of transducers. Four SPI lines (MISO, MOSI, SCK, and SS) are included to communicate between front-end and back-end in case the front-end needs digitally controlled blocks. Two clock lines are provided (CLK1 and CLK2), ready to be supplied if required. Finally, Pull Down and Detect (PD and DET) are required for detecting whether the port is connected to a front-end module. On the back-end side, the PD pin is connected to ground, and DET pin is both connected to the power supply through a pull-up resistor and to a general-purpose input on the central control of the back-end. By default, the voltage on DET is high while once the port is connected, the voltage DET goes down, indicating the successful connection to the front-end.

D. Core

The core is the last module of the proposed system. It carries out data analysis with software customized to fit the target biological compound. The core is based on a Raspberry Pi (RPi) 3 Model B, as the RPi contains high-performance Quad-core CPUs that can execute complex tasks and algorithms for data analysis and processing. A smart data analysis block carries out data analysis using the relationship between the input and output electrical signals. The RPi also contains a Wi-Fi module to connect the biosensing device to the cloud for IoT applications. In the core, a Cloud IoT Interface sub-block is included not only to store the sensor-related data into the cloud but also to provide an interface to other cloud services for IoT applications. The Raspbian Operating System (OS) provides the needed software development environments. A C++ based software is developed in Qt Creator to communicate with the back-end through the serial port and to provide the user (device developer) an environment where he can create specific processing software routines. A new custom library with different software classes is also included to implement standard features in biosensing devices, such as the need to excite voltage waveform for voltammetry or to sample the potential at the input.

IV. Example of Device Implementation

Fig. 3 shows the custom front-end A for amperometric sensing, the custom front-end B for potentiometric sensing, and the custom front-end C for memristive sensing, which interface to here presented system. All these front-ends are compatible with the primary objective of this work, they are interchangeable, and they can be connected to the same common back-end. The here presented front-ends display examples of possible device implementation. This work shows that new

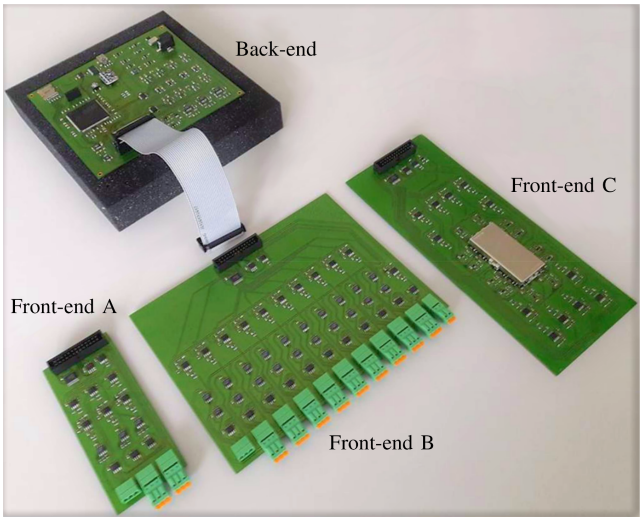

Fig. 3. Prototype of biosensing devices. Custom front-end A for amperometric sensing, front-end B for potentiometric sensing, and front-end C for memristive sensing can be connected to the same back-end. New and diverse front-end can be built and add with our approach.

front-ends could be quickly built by biosensor developers to target other biological compounds, just retracing the steps delineated in this paper. The three devices are tested to demonstrate the capability and flexibility of the approach proposed in this work. The design of the front-end heavily depends on the sensor type and the corresponding application. The output electrical signals coming from the biochemical transducer are converted to voltage signals through the sensor front-end and then are connected to the input of a 16-to-1 multiplexer to allow multiple sensor arrays. In the amperometric sensor, the custom front-end A contains a Trans-Impedance Amplifier (TIA), filtering and level shifting blocks. The detailed design of each block can be found in [19]. The proposed front-end B features a voltage buffer and a filter to target ion in the potentiometric sensor. The design of the voltage buffer block is in [22], and the filtering block is in [19]. In the memristive sensor, the custom front-end C is composed of a TIA and filter blocks. The detailed design of TIA has presented in [27], and the filtering block shares its design to front-end B.

A W25Q80JVSNIQ SPI-Flash memory is added in every front-end to store test parameters and electronic biosensor circuit information. It has a memory size of $8\,\mathrm{Mb}$ with a clock frequency of $133\,\mathrm{MHz}$. The 16-to-1 multiplexer accepts sixteen independent measurement signals coming from the electronic biosensors, which are sufficient for the majority of the biosensing applications. For the multiplexer, a CD74HC4067SM96 chip is used because of its low switching time and on-state resistance. In the software running on the core, a flexible Graphical User Interface (GUI) is developed to display the data processing performed by the core and outcoming the results. The GUI is later customized to fit the three different implemented biosensors. The amperometric sensing, Chrono Amperometry (CA), Cyclic Voltammetry (CV) and Differential Pulse Voltammetry (DPV) are included and available in the GUI. In this work, the data obtained by CV measurements are fully reported to demonstrate the generality

of the approach. In the potentiometric sensor, the GUI panel shows options for selecting how many and which input channels are used for the measurement, triggering the sampling of the corresponding channel. In the memristive sensor, start voltage, step voltage, sweep time and end voltage are set by the user to drive the back-end in different experimental conditions.

V. Materials and Methods

To verify the effectiveness of the developed system, the approach is validated by testing three biosensing devices designed as examples, as new fully functioning biosensor prototypes. The three devices are based on three different previously-proposed biosensing principles. These biosensors are selected since they provide a wide range of applications, with various specific working principles, functions and internal structures, hence, being optimal as a capable demonstrator of our approach.

A. Amperometric sensor

The electrochemical sensor in this experiment resembles [28], and it is presented in Fig 4. A Pencil Graphite Electrode (PGE) as Working Electrode (WE), a K0265 Ag/AgCl electrode from Ametek Scientific Instruments as Reference Electrode (RE) and a Pt wire as Counter Electrode (CE), forms a three-electrode electrochemical cell. Namely, the PGE is the tip of a Staedtler Mars Lumograph Wood Pencil 3H, and it is made up of a composite material containing graphite, clay and wax. The two extremities of the pencil have been peeled to obtain from one side the WE active area ($12.6\,\mathrm{mm}^2$) and from the other side the electronic connection with the system mentioned above parts to obtain the electronic biosensor. Further details are present in [28].

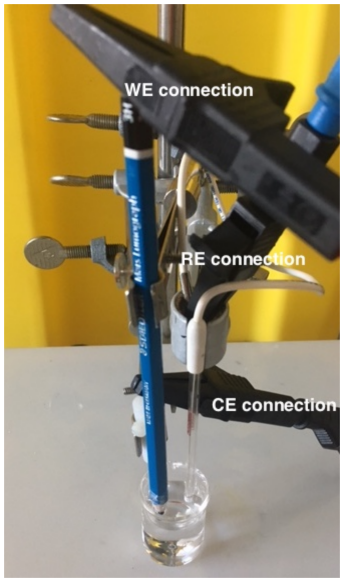

Fig. 4. Amperometric sensor setup, pencil graphite WE, Ag/AgCl RE, and Pt wire CE.

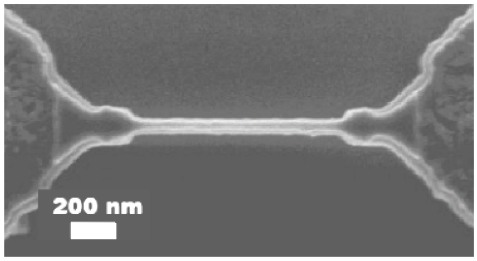

(a)

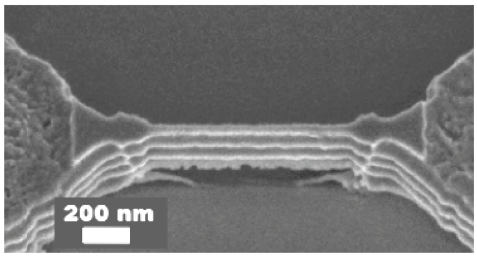

(b)

Fig. 5. SEM picture of the fabricated memristive silicon-wire devices, top view (a) and tilted view (b).

B. Potentiometric sensor

Platinum-WE Screen Printed Electrodes (SPE) with WE of diameter $4\,\mathrm{mm}$ are purchased from DropSens (Spain). Platinum nanostructured solid-contacts are produced by electrochemical means [29]. Consequently, $100\,\mathrm{mg}$ of lithium membrane cocktail consisting of $28.0\,\mathrm{wt}\%$ Poly(vinyl chloride) high molecular weight, $1.0\,\mathrm{wt}\%$ Li Ionophore VI, $0.7\,\mathrm{wt}\%$, Potassium tetrakis(4-chlorophenyl)borate, and $70.3\,\mathrm{wt}\%$ 2-Nitrophenyl octyl ether was dissolved in $1\,\mathrm{ml}$ of Tethraydrofuran (THF). This solution is drop-cast on each electrode in a volume of $10\,\mu\mathrm{l}$. All the chemicals are purchased from Sigma Aldrich.

C. Memristive sensor

Memristive silicon-wire devices are fabricated for this work through a top-down fabrication process utilizing Electron Beam (E-Beam) lithography and Deep Reactive Ion Etching (DRIE) processes [30]. Fig. 5 displays the fabricated memristive device. The wires are suspended and anchored between Nickel Silicide (NiSi) pads that serve to the electrical characterization. Those pads are defined through E-Beam lithography and fabricated through Nickel (Ni) evaporation followed by lift-off and annealing procedures. For achieving successful integration of the sensing chip with electronics, extension metal lines are introduced on top of the already fabricated devices forming a 12-wire platform sharing a common source and demonstrating individual drains. The $(1 \times 1)\,\mathrm{cm}^2$ chip consisting of memristive devices, is thereafter wire-bonded on a specially designed chip-holder that can be easily plugged using board-to-board connectors to the main PCB allowing a flexible and robust sensing procedure. Further details are present in [30], [25].

VI. Results and Discussion

All the three devices implemented as examples of biosensing devices are tested, and the results are compared to the state-of-the-art and to commercial lab instruments to prove the efficiency of our approach.

A. Results of amperometric sensor

7-point CV calibration is carried out on Acetaminophen (APAP) drug dissolved in a Phosphate Buffered Saline (PBS) as background electrolyte to verify the performance of our amperometric sensor developed as a standalone device with the proposed approach. A staircase voltage between $-0.1\,\mathrm{V}$ and $1.1\,\mathrm{V}$ is applied on the electrochemical cell by the back-end and the faradaic current is sampled back by the back-end. The calibration line obtained by the six increasing concentrations of APAP is compared with the one obtained using a commercial lab instrument, the potentiostat Metrohm Autolab PGSTAT 302N driven by the software Nova 11.1, in the same conditions. Fig. 6(a) and Fig. 6(b) present the voltammogram acquired by our board and the lab instrument, respectively. They present differences in the shape related to the different electronic system used to acquire the signals. While differences on the CV are visible, the two calibration lines, which are the real output of the sensor, are highly comparable as shown in Fig. 6(c), while our device present higher sensitivity with respect to the commercial instrument ($1 \times 10^{-7}\,\mathrm{A\,\mu M^{-1}}$ for our system and $5 \times 10^{-8}\,\mathrm{A\,\mu M^{-1}}$ for the commercial instrument).

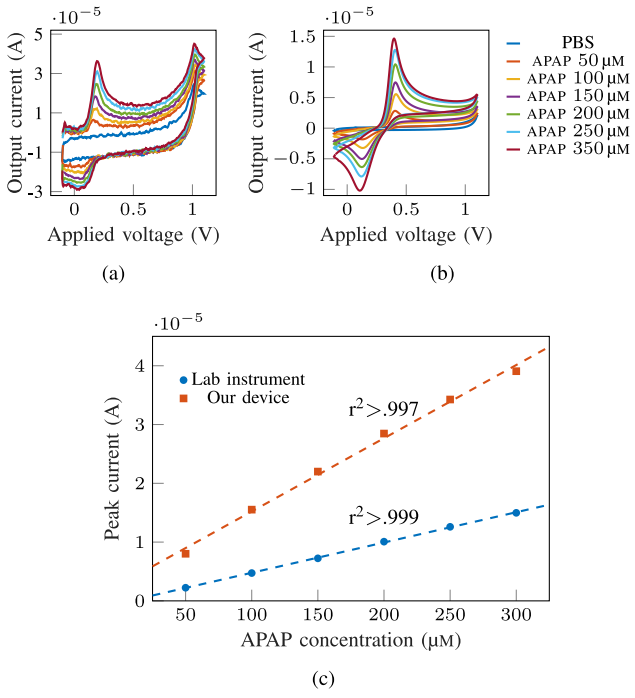

Fig. 6. Output voltammogram acquired by our device (a) and by the commercial lab instrument (b), with comparison between resulting calibration curves (c).

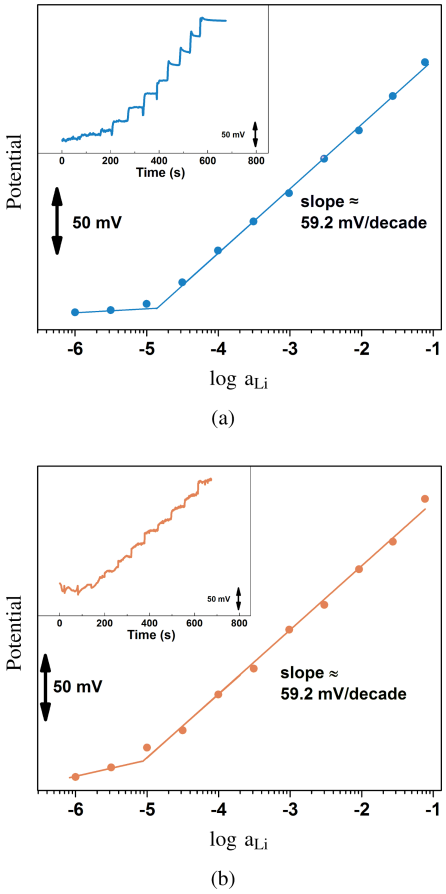

Fig. 7. Comparison of lithium-ion detection with a commercial potentiostat (a) and with our device (b). The small insets show the time trace during successive solute additions, while the main graphs display the corresponding calibration curves.

B. Results of potentiometric sensor

Potentiometric experiments are carried out with the ion-sensitive device, interfacing the front-end with previously developed all-solid-state ion-selective sensors based on nanostructured platinum contacts [29]. Fig. 7 reports the results in comparison with a commercial potentiostat (Metrohm Autolab PGSTAT 302N) driven by the software Nova 1.11. It is possible to observe that in both cases, very smooth and stable responses are obtained with quasi-Nernstian slope. From the small insets showing the time trace during successive solute additions, it is evident that the proposed electronic device offers sharper steps, with lower potential drift, especially at high concentrations. Besides, a slightly lower Limit of Detection (LOD) is achieved with our device with respect to the commercial instrument ($8.5 \times 10^{-6}\,\mathrm{M}$ vs $1.3 \times 10^{-5}\,\mathrm{M}$).

C. Results of memristive sensor

The hysteresis loop characterizes the electrical response of the memristive devices. The charge carriers rearrange at the nanoscale while perturbated by external the applied voltage bias producing the memory effect. The hysteresis is pinched very close to zero voltage for most of the bare nanowire devices due to the effect of external conditions, such as the ambient humidity. While, usually, the fully-pinched hysteresis is

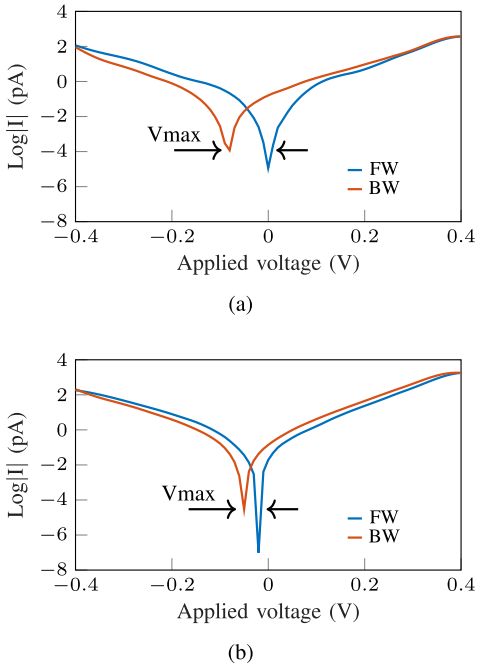

Fig. 8. Voltage gaps measured by our device in forward scan (FW) and backward scan (BW), considering concentrations of 3.3 fM (a) and 330 fM (b) of PSA.

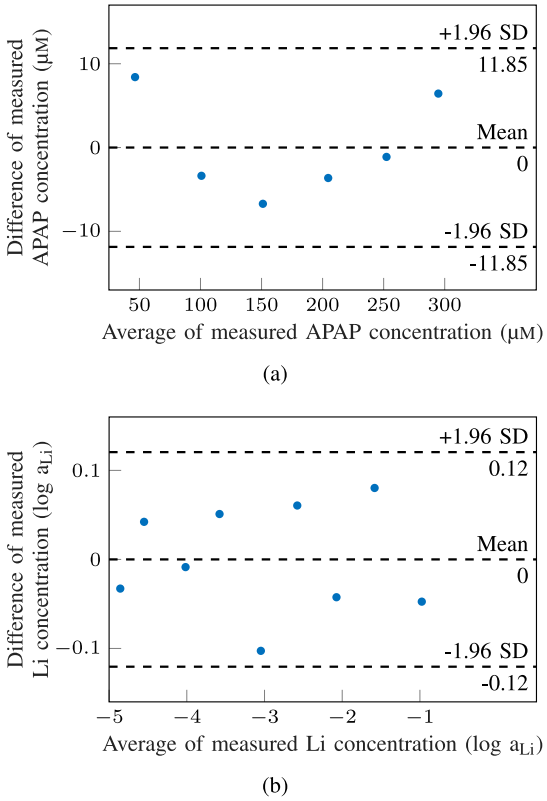

Fig. 9. Bland–Altman representation of results. The differences between values obtained by our device and lab instrument are plotted against their mean, considering the measured concentration of APAP for amperometric sensor (a), and concentration of Lithium for potenziometric sensor (b).

then lost during bio-detection. Fig. 8 shows acquisitions done for the different concentrations of PSA. As the concentration increases, the maximum voltage gap decreases.

D. Results of the approach

The experimental results prove the capability of the proposed approach. All three biosensing devices show performance comparable with literature, with the advantage of being obtained by the same common generalized platform. Namely, our amperometric sensing-based device achieves a sensitivity value comparable with respect to [19], [20], [28]. Our potentiometric sensor shows a LOD $50\,\%$ lower with respect to [29], and our memristive device presents similar behaviour to [25].

In Fig. 9, the results of our devices are compared to the standard lab instruments using the Bland–Altman plot, considering both APAP detection in Fig. 9(a) and Lithium sensor in Fig. 9(b). Both sensors do not present a visible bias with respect to the lab instrument since the mean of differences is many orders of magnitude lower than the standard deviation. The largest differences obtained were $+8.4/-6.7\,\mu\text{M}$ and $+0.08/-0.10\,\log a_{\text{Li}}$ in amperometric and potentiometric devices, respectively. In both cases, the results fall under the 95% limits of, which is computed as 1.96 times the standard deviation of measurement differences. These results certify that in the presented examples, our system does not present loss in accuracy when measuring the concentration of analyte with respect to the lab instrument.

The use of our approach is successful in terms of optimization of experimental activities. The common back-end notably accelerates the development process. The results demonstrate that it is possible to share this common backbone, thus avoiding the need to spend time and effort on its implementation. The tested devices are enough diversified to cover most of the aspects required for the extraction of signals, including their transmission, and their final elaboration. The reduced effort that has to be invested in the implementation of non-specific electronics is evident from the experimental result.

VII. Conclusion

We presented a new approach to develop biosensing devices through a multiple-purpose system to help designers in the fast implementation of new bioelectronics systems, focusing only on the part of the design which is specific to the target-molecule, in all the application where commercially available systems are not suitable, like portable, low-power, or low-cost devices. In this regard, our new approach made it possible to assemble a new biosensor creating only a custom front-end and writing firmware/software while the rest of the system can be fully shared. From the experimental results, considering three completely different biosensors, we have demonstrated that our approach can successfully increase generalization in the fields of biosensing technology. In the future steps, the proposed system will be freely shared as open hardware and open software to all the scientific community.

ACKNOWLEDGMENT

The authors would like to thank T. Kilic for her valuable suggestions in some experiments.

REFERENCES

[1] N. Bhalla, P. Jolly, N. Formisano, and P. Estrela, "Introduction to biosensors," *Essays in biochemistry*, vol. 60, no. 1, p. 8, 2016.

[2] F.-G. Banica, *Chemical sensors and biosensors: fundamentals and applications*. John Wiley & Sons, 2012.

[3] C. Dincer, R. Bruch, E. Costa-Rama, M. T. Fernández-Abedul, A. Merkoçi, A. Manz, G. A. Urban, and F. Güder, "Disposable sensors in diagnostics, food, and environmental monitoring," *Advanced Materials*, vol. 31, no. 30, p. 1806739, 2019.

[4] S. Sang, W. Zhang, and Y. Zhao, "State of the art in biosensors-general aspects," in *Review on the design art of biosensors*, T. Rinken, Ed. Intech, 2013, pp. 89–110.

[5] A. J. Bard, L. R. Faulkner, J. Leddy, and C. G. Zoski, *Electrochemical methods: fundamentals and applications*. wiley New York, 1980, vol. 2.

[6] Y. Q. Fu, J. Luo, N.-T. Nguyen, A. Walton, A. J. Flewitt, X.-T. Zu, Y. Li, G. McHale, A. Matthews, E. Iborra *et al.*, "Advances in piezoelectric thin films for acoustic biosensors, acoustofluidics and lab-on-chip applications," *Progress in Materials Science*, vol. 89, pp. 31–91, 2017.

[7] R. B. Schasfoort, *Handbook of surface plasmon resonance*. Royal Society of Chemistry, 2017.

[8] S. A. Pidenko, N. A. Burmistrova, A. A. Shuvalov, A. A. Chibrova, Y. S. Skibina, and I. Y. Goryacheva, "Microstructured optical fiber-based luminescent biosensing: Is there any light at the end of the tunnel?-a review," *Analytica Chimica Acta*, vol. 1019, pp. 14–24, 2018.

[9] S. M. Spivak and F. C. Brenner, *Standardization essentials: Principles and practice*. CRC Press, 2018.

[10] A. Meddeb, "Internet of things standards: who stands out from the crowd?" *IEEE Communications Magazine*, vol. 54, no. 7, pp. 40–47, 2016.

[11] K. H. Gilchrist, V. N. Barker, L. E. Fletcher, B. D. DeBusschere, P. Ghanouni, L. Giovangrandi, and G. T. Kovacs, "General purpose, field-portable cell-based biosensor platform," *Biosensors and Bioelectronics*, vol. 16, no. 7-8, pp. 557–564, 2001.

[12] A. Bonanno, A. Sanginario, S. Marasso, B. Miccoli, K. Bejtka, S. Benetto, and D. Demarchi, "A multipurpose CMOS platform for nanosensing," *Sensors*, vol. 16, no. 12, p. 2034, 2016.

[13] T. Arévalo-Ramírez, C. C. Torres, A. C. Rosero, and P. Espinoza-Montero, "Low cost potentiostat: Criteria and considerations for its design and construction," in *2016 IEEE ANDESCON*, Arequipa, 2016, pp. 1–4.

[14] M. D. Dryden, R. Fobel, C. Fobel, and A. R. Wheeler, "Upon the shoulders of giants: open-source hardware and software in analytical chemistry," *Analytical chemistry*, vol. 89, no. 8, pp. 4330–4338, 2017.

[15] S. D. Adams, E. H. Doeven, K. Quayle, and A. Z. Kouzani, "Ministat: Development and evaluation of a mini-potentiostat for electrochemical measurements," *IEEE Access*, vol. 7, pp. 31 903–31 912, 2019.

[16] M. D. M. Dryden and A. R. Wheeler, "Dstat: A versatile, open-source potentiostat for electroanalysis and integration," *PLOS ONE*, vol. 10, no. 10, pp. 1–17, 2015.

[17] R. Fisher, L. Ledwaba, G. Hancke, and C. Kruger, "Open hardware: A role to play in wireless sensor networks?" *Sensors*, vol. 15, no. 3, pp. 6818–6844, 2015.

[18] G. Ozcelikay, L. Karadurmus, S. I. Kaya, N. K. Bakirhan, and S. A. Ozkan, "A review: New trends in electrode systems for sensitive drug and biomolecule analysis," *Critical Reviews in Analytical Chemistry*, pp. 1–14, 2019.

[19] F. Stradolini, A. Tuoheti, P. Motto Ros, D. Demarchi, and S. Carrara, "Raspberry Pi based system for portable and simultaneous monitoring of anesthetics and therapeutic compounds," in *2017 New Generation of CAS (NGCAS)*, Genova, 2017, pp. 101–104.

[20] S. Aiassa, F. Stradolini, A. Tuoheti, S. Carrara, and D. Demarchi, "Quasi-digital biosensor-interface for a portable pen to monitor anaesthetics delivery," in *2019 15th Conference on Ph.D Research in Microelectronics and Electronics (PRIME)*, Lausanne, 2019, pp. 265–268.

[21] S. Aiassa, S. Carrara, and D. Demarchi, "Optimized sampling rate for voltammetry-based electrochemical sensing in wearable and IoT applications," *IEEE Sensors Letters*, vol. 3, no. 6, pp. 1–4, June 2019.

[22] I. Ny Hanitra, L. Lobello, F. Stradolini, A. Tuoheti, F. Criscuolo, T. Kilic, D. Demarchi, S. Carrara, and G. De Micheli, "A flexible front-end for wearable electrochemical sensing," in *2018 IEEE International Symposium on Medical Measurements and Applications (MeMeA)*, Rome, 2018, pp. 1–6.

[23] I. Ny Hanitra, F. Criscuolo, S. Carrara, and G. De Micheli, "Multi-target electrolyte sensing front-end for wearable physical monitoring," in *2019 15th Conference on Ph.D Research in Microelectronics and Electronics (PRIME)*, Lausanne, 2019, pp. 249–252.

[24] M. Cuartero, M. Parrilla, and G. A. Crespo, "Wearable potentiometric sensors for medical applications," *Sensors*, vol. 19, no. 2, p. 363, 2019.

[25] I. Tzouvadaki, P. Jolly, X. Lu, S. Ingebrandt, G. De Micheli, P. Estrelaand, and S. Carrara, "Label-free ultrasensitive memristive aptasensor," *Nano Letters*, vol. 16, no. 7, p. 4472–4476, 2016.

[26] M. Rajabzadeh, D. Djekic, M. Haeberle, J. Becker, J. Anders, and M. Ortmanns, "Comparison study of integrated potentiostats: Resistive-TIA, capacitive-TIA, CT $\sigma\delta$ modulator," in *2018 IEEE International Symposium on Circuits and Systems (ISCAS)*, Florence, 2018, pp. 1–5.

[27] I. Tzouvadaki, A. Tuoheti, G. De Micheli, D. Demarchi, and S. Carrara, "Portable memristive biosensing system as effective point-of-care device for cancer diagnostics," in *2018 IEEE International Symposium on Circuits and Systems (ISCAS)*, Florence, 2018, pp. 1–5.

[28] F. Stradolini, A. Tuoheti, T. Kilic, S. Ntella, N. Tamburrano, Z. Huang, G. De Micheli, D. Demarchi, and S. Carrara, "An IoT solution for on-line monitoring of anesthetics in human serum based on an integrated fluidic bio-electronic system," *IEEE Transactions on Biomedical Circuits and Systems*, vol. 12, no. 5, pp. 1056–1064, 2018.

[29] F. Criscuolo, I. Taurino, F. Stradolini, S. Carrara, and G. De Micheli, "Highly-stable Li+ ion-selective electrodes based on noble metal nanostructured layers as solid-contacts," *Analytica Chimica Acta*, vol. 1027, pp. 22–32, 2018.

[30] I. Tzouvadaki, C. Parrozzani, A. Gallotta, G. De Micheli, and S. Carrara, "Memristive biosensors for psa-igm detection," *BioNanoScience*, vol. 5, no. 4, pp. 189–195, 2015.